Sensing Picornaviruses Using Molecular Imprinting Techniques on a Quartz Crystal Microbalance

ARTICLE *in* ANALYTICAL CHEMISTRY · JUNE 2009

Impact Factor: 5.64 · DOI: 10.1021/ac8019569 · Source: PubMed

8 AUTHORS, INCLUDING:

R. Schirhagl
University of Groningen
37 PUBLICATIONS **537** CITATIONS
SEE PROFILE

Oliver Hayden
Siemens
74 PUBLICATIONS **2,951** CITATIONS
SEE PROFILE

Peter Lieberzeit
University of Vienna
109 PUBLICATIONS **1,482** CITATIONS
SEE PROFILE

Dieter Blaas
Medical University of Vienna
186 PUBLICATIONS **6,409** CITATIONS
SEE PROFILE

Anal. Chem. **2009,** *81,* 5320–5326

Sensing Picornaviruses Using Molecular Imprinting Techniques on a Quartz Crystal Microbalance

Michael Jenik,[†] Romana Schirhagl,[†] Christian Schirk,[†] Oliver Hayden,[†] Peter Lieberzeit,[†] Dieter Blaas,[‡] Guntram Paul,[§] and Franz L. Dickert*[,†]

Department of Analytical Chemistry and Food Chemistry, University of Vienna, Waehringer Strasse 38, 1090 Vienna, Austria, Department of Medical Biochemistry, Medical University of Vienna, Dr.-Bohrgasse 9, 1030 Vienna, Austria, and Intervet International GmbH, Osterather Strasse 1A, 50739 Köln, Germany

Molecular imprinting techniques were adapted to design a sensor for the human rhinovirus (HRV) and the foot-and-mouth disease virus (FMDV), which are two representatives of picornaviruses. Stamp imprinting procedures lead to patterned polyurethane layers that depict the geometrical features of the template virus, as confirmed by AFM for HRV. Quartz crystal microbalance (QCM) measurements show that the resulting layers incorporate the template viruses reversibly and lead to mass effects that are almost an order of magnitude higher than those of nonspecific adsorption. Thus, for example, the sensor yields a net frequency effect of −300 Hz when applying a virus suspension with a concentration of ∼100 μg/mL with an excellent signal-to-noise ratio. The cavities are not only selective to shape but also to surface chemistry: different HRV serotypes (HRV1A, HRV2, HRV14, and HRV16, respectively) can be distinguished with the sensor materials by a selectivity factor of 3, regardless of the group (major/minor) to which they belong. The same selectivity factor can be observed between HRV and FMDV. Hence, imprinting leads to an "artificial antibody" toward viruses, which does not only recognize their receptor binding sites, but rather detects the whole virus as an entity. Brunauer−Emmett−Teller (BET) studies allow simulation of the sensor characteristics and reveal the number of favorable binding sites in the coatings.

Picornaviruses constitute a family of viruses having in common icosahedral shape with an outer protein capsid and an RNA strand in their centers and encompassing some of the most important human and animal pathogens. Typical examples are the human rhinovirus (HRV) or the foot-and-mouth-disease virus (FMDV). The former has a diameter of 30 nm and a molecular mass of $\sim 8.5 \times 10^6$ g/mol, whereas FMDV is smaller by 5 nm. HRV is composed of 60 copies of each of four different capsid proteins,[1] as well as the RNA genome.[2] Currently, more than 100 different serotypes are known,[3] which can mainly be divided into two groups: the majority of all HRV (major group HRV, 91 serotypes) bind to the so-called intracellular adhesion molecule 1 (ICAM-1)[4] in the human body, whereas 10 serotypes (minor group HRV) bind to the low-density lipoprotein receptor (LDL-R).[5] The sole exception from this scheme is HRV87, because it does not use either of the previously mentioned receptors. However, X-ray analysis[6] has shown that aside of the receptor region, intergroup similarity does not exceed intragroup similarity. Therefore, the arrangements of the respective virus surface proteins of species belonging to the same group differ among each other[7] to the same extent as that between the groups. Based on this knowledge, one can think about artificial recognition materials for determining not only HRV as such, but also differentiating between different serotypes. Therefore, the main objective is the synthesis of a material that interacts with the entire capsid rather than only the receptor site, as would be the case in biological recognition. A very straightforward way for achieving this goal is molecular imprinting:[8] here, one can design functionalized materials that are able to interact noncovalently with the analyte,[9,10] leading to an artificial antibody[11] for the rhinovirus in the ideal case. The earliest successful attempt for bioanalyte imprinting covered emulsion-polymerized beads templated with bacteria on the interphase.[12] During our work in bioanalyte sensing, it has been proven most useful to synthesize a cross-linked polymer that contains highly selective recognition sites by the means of soft-lithographic

* To whom correspondence should be addressed. Fax: +43/2243/3627315. E-mail: franz.dickert@univie.ac.at.

† Department of Analytical Chemistry and Food Chemistry, University of Vienna.

‡ Department of Medical Biochemistry, Medical University of Vienna.

§ Intervet International GmbH.

(1) Ledford, R. M.; Patel, N. R.; Demenczuk, T. M.; Watanyar, A.; Herbertz, T.; Collett, M. S.; Pevear, D. C. *J. Virol.* **2004**, *78*, 3663–3674.

(2) Verdaguer, N.; Blaas, D.; Fita, I. *J. Mol. Biol.* **2000**, *300*, 1179–1194.

(3) Uncapher, C. R.; Dewitt, C. M.; Colonno, R. J. *Virology* **1991**, *180*, 814–817.

(4) Greve, J. M.; Davis, G.; Meyer, A. M.; Forte, C. P.; Yost, S. C.; Marlor, C. W.; Kamarck, M. E. *Cell* **1989**, *56*, 859–847.

(5) Vlasak, M.; Roivainen, M.; Reithmayer, M.; Goesler, I.; Laine, P.; Snyers, L.; Hovi, T.; Blaas, D. *J. Virol.* **2005**, *79*, 7389–7395.

(6) Verdaguer, N.; Fita, I; Reithmayer, M.; Moser, R.; Blaas, D. *Nature Struct. Mol. Biol.* **2004**, *11*, 429–434.

(7) Vlasak, M.; Blomqvist, S.; Hovi, T.; Hewat, E; Blaas, D. *J. Virol.* **2003**, *77*, 6923–6930.

(8) Dickert, F. *Anal. Bioanal. Chem.* **2007**, *389*, 353–354.

(9) Dickert, F. L.; Hayden, O.; Lieberzeit, P.; Haderspoeck, C.; Bindeus, R.; Palfinger, C.; Wirl, B. *Synth. Met.* **2003**, *138*, 65–69.

(10) Belmont, A. S.; Jaeger, S.; Knopp, D.; Niessner, R.; Gauglitz, G.; Haupt, K. *Biosens. Bioelectron.* **2007**, *22*, 3267–3272.

(11) Hayden, O.; Lieberzeit, P. A.; Blaas, D.; Dickert, F. L. *Adv. Funct. Mater.* **2006**, *16*, 1269–1278.

(12) Alexander, C; Vulfson, E. N. *Adv. Mater.* **1997**, *9*, 751–755.

10.1021/ac8019569 CCC: $40.75
Published on Web 05/26/2009

approaches.[13] In combination with mass-sensitive transducers, such as quartz crystal microbalances (QCMs), molecularly imprinted polymers (MIP) lead to very appreciable sensor systems, which also allows for selective detection of the template virus, such as, for example, the tobacco mosaic virus (TMV),[14] even in crude plant saps.[15] Hence, implementing bioanalogous selectivity in an artificial material is of special interest in analysis, because it would allow natural materials with their somewhat limited ruggedness to be avoided. Furthermore, virus MIPs indeed open up the way to selective rapid analysis of these species, which are otherwise only accessible via microbiological analysis protocols. In terms of materials science, the picornaviruses furthermore allow for assessing the influence of surface chemistry of the individual analyte on the respective sensor responses, because the shapes of all HRVs are the same, independent of the serotype. Furthermore, the minor difference in diameter by 5 nm between HRV and FMDV can be analyzed with respect to biorecognition by MIPs. To complement the physicochemical picture of this extraction process by MIP-coated QCMs, the adsorption phenomena that are occurring can be quantified via the respective Brunauer−Emmett−Teller (BET) adsorption isotherm.

EXPERIMENTAL SECTION

We purchased chemicals from Merck and Sigma−Aldrich in analytical grade or the highest available synthetical grade and used them as received. HRV suspensions were provided by D. Blaas, and suspensions of deactivated foot-and-mouth disease virus were provided by Intervet. For the synthesis of the polyurethane MIPs, we mixed the monomer compounds Bisphenol A (2,2-bis-(4-hydroxyphenyl)-propane), Tris (2-amino-2-hydroxymethyl-1,3-propanediol·HCl) (23.4 mg), Phloroglucinol (1,3,5-trihydroxybenzene) (28.0 mg), and 4,4′-isocyanato-diphenyl-methane (48.6 mg), diluted with 100 μL tetrahydrofurane (THF) and prepolymerized at 70 °C for ∼10 min in the presence of catalytic amounts of pyridine. In this approach, phloroglucinol acted as the cross-linker ensuring flat and firm layers hence with reduced swelling behavior during the measurements. We then applied this prepolymer mixture onto a QCM via spin coating. For this purpose, we pipetted 15 μL onto the device and spun it off at 3000 rpm to obtain layers in the range of 250−350 nm thick.

In parallel to synthesizing these layers, we prepared the template stamps. For this purpose, we applied a diluted virus suspension in 10 mM Tris (pH 7.2) that contained a concentration of ∼1 mg/mL HRV to obtain a monolayer of adsorbed viruses on the stamp substrate, which was a glass disk with dimensions of 5 mm × 5 mm. To do so, we placed 3 μL of the suspension on the substrate and incubated at 4 °C for 30 min. Afterward, we spun off the stamp at 2000 rpm to remove excess solution and, thus, avoid the formation of buffer crystals. During incubation, the viruses adsorb on the glass through polar interactions and therefore remain adhered to it, even after spinning. To prevent covalent binding between the hydroxyl groups of the viruses and the isocyanate groups of the polymer, we used a modifier. For this purpose, we spin-coated the stamp with a 10 mM solution of phloroglucinol and phenylendiamine in THF. After this, we immediately pressed the stamp into the polymer material and then hardened for 24 h at room temperature. To lift off the stamp, we stirred the QCM in temperate water (∼40 °C) and subsequently rinsed with 0.5 M HCl to denature the viruses[16] and, hence, detach them from the polymer.[17]

QCM were based on AT-cut quartz disks with a diameter of 15.5 mm, a thickness of 168 μm, and a resonance frequency of 10 MHz. Two electrode pairs, each with a diameter of 5 mm, were generated on quartz blanks using a screen-printing procedure, as described previously.[18] This dual electrode design with a MIP and a nonimprinted reference material eliminates unspecific effects that may be caused by temperature fluctuations, viscosity, etc. We performed all sensor measurements in a custom-made measuring cell with a 15-μL volume cast with polydimethyl siloxane (PDMS) operated in stopped-flow mode at a measuring temperature of 25 °C. The QCM electrodes were connected to an oscillator circuit and, this to, a frequency counter (Agilent 53131A) read out by custom-made software via a GPIB USB interface.

We recorded all AFM images on a Veeco Nanoscope IVa system in contact mode with Veeco SNL-10 silicon tips with a spring constant of 40 N m and an onset pressure corresponding to a differential signal of 1 V on the photo diode. To obtain an image, we mounted the substrate that contained the imprint onto a sample disk and scanned with scan rates in the range of 1−2 Hz at room temperature. To confirm the virus particle concentration, we counted the viruses in AFM images. For this purpose, we deposited a defined volume of a virus suspension onto a glass substrate of defined size spin coated with the polyurethane previously described, to guarantee a flat surface. The polymer fully absorbed the solvent buffer, leaving behind the viruses on the surface, which can directly be counted. These measurements revealed an accuracy of better than 20%.

RESULTS AND DISCUSSION

AFM Studies. The first step in bioanalyte layer design is ensuring that the stamping procedures indeed generate cavities in the polymer matrix. Figure 1 shows AFM images of different polymer layers, both imprinted and nonimprinted ones. Figure 1a depicts the surface of a nonimprinted polyurethane layer that has been been synthesized from the same monomer mixture as the MIPs. Evidently, spin coating, in this case, leads to outstandingly flat surfaces: the length of the vertical axis, in this case, is 12 nm; therefore, the surface roughness is in the range of 2−3 nm. Figure 1b, on the other hand, shows a surface with a self-organized HRV monolayer. The overall height, in this case, is somewhat lower than expected, because the viruses are tightly packed and, hence, the AFM tip does not touch the substrate surface. However, the lateral dimensions clearly represent HRV virions. Furthermore, Figure 1c depicts a surface after imprinting and partly washing off the template viruses. For better visibility,

(13) Lieberzeit, P. A.; Glanznig, G.; Jenik, M.; Gazda-Miarecka, S.; Dickert, F. L.; Leidl, A. *Sensors* **2005**, *5*, 509–518.

(14) Bolisay, L. D.; Culver, J. N.; Kofinas, P. *Biomacromolecules* **2007**, *8*, 3893–3899.

(15) Dickert, F. L.; Hayden, O.; Bindeus, R.; Mann, K. J.; Blaas, D.; Waigmann, E. *Anal. Bioanal. Chem.* **2004**, *378*, 1929–1934.

(16) Hughes, J. H.; Thomas, D. C.; Hamparian, V. V. *Proc. Soc. Exp. Biol. Med.* **1973**, *144*, 555–560.

(17) Giranda, V. L.; Heinz, B. A.; Oliveira, M. A.; Minor, I.; Kim, K. H.; Kolatkar, P. R.; Rossmann, M. G.; Rueckert, R. R. *Proc. Natl. Acad. Sci. U.S.A.* **1992**, *89*, 10213–10217.

(18) Dickert, F. L.; Hayden, O. *Anal. Chem.* **2002**, *74*, 1302–1306.

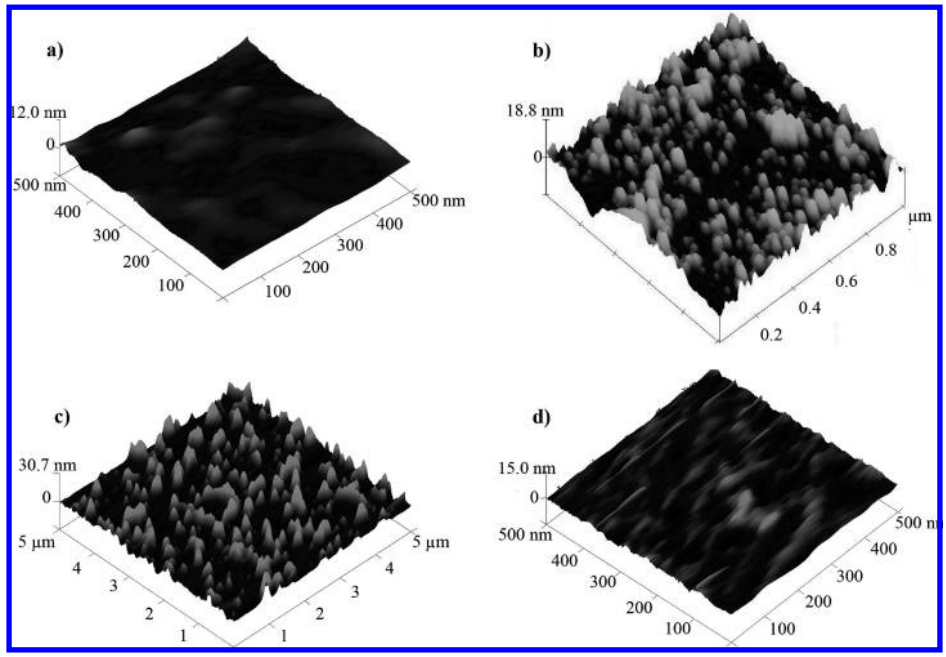

Figure 1. Contact mode AFM images of polyurethane layers: (a) nonimprinted polymer, (b) HRV self-assembled on a surface, (c) MIP with partially removed template, and (d) MIP after washing.

the scale in the *z*-dimension between Figures 1b and 1c is different (18.8 nm versus 30 nm), because, in the latter case, the tip may touch the polymer surface. The large "bumpy" features to be seen are ~30 nm high, which corresponds very well with the dimensions of the HRV. However, the lateral dimensions vary much more and range from ~30 nm (i.e., a single virus), up to some hundreds of nanometers, which suggests the formation of larger virus clusters on the polymer surface due to interaction between the virions. Only the lateral dimensions of the surface features being are larger than expected, but not the vertical ones; this is already a strong indicative of successful imprinting. Obviously, any virions that belong to a "second layer" of HRV on the MIP surface are easily washed away, whereas the particles in contact with the polymer surface remain bound.

Finally, the AFM image in Figure 1d shows a MIP surface after all template viruses have been washed off. The difference toward the nonimprinted material is obvious: the surface roughness is higher and reaches levels of 6−7 nm, with the diameters of individual flat hollows in the range from 25 nm to ~100 nm. This observation is consistent with two facts: (i) the aforementioned clustering of viruses on the MIP surface and (ii) that imprinted cavities resulting from biospecies are usually shallower than half their respective diameter. Furthermore, the space between the cavities shows elevated "bumps" of polymeric material, which is understandable, given the stamping procedure: here, a forming polymer matrix is "pushed" aside by the species on the template stamp, thus filling in the gaps between the individual viruses. This also explains why cavities must be shallow: if they become too deep, the polymer might fill the interstitial space between the stamp surfaces and the (idealized) virus monolayer, thus generating "cages", from which the template can no longer be removed without fully destroying it. The entrance to the cavity would also be too narrow for reincorporation of the respective virus. Hence, the dimensions of both the cavities and elevations in the images meet the HRV dimensions very well and, thus, strongly support that the surface imprinting approach has been successful. Consequently, these AFM studies represent the basis for further investigations that concern the recognition behavior of the MIPs: in mass-sensitive sensing, of course a geometrical as well as chemical fit between the layer and the template is necessary for leading to a noncovalent interaction network.

HRV QCM Sensor Responses. Therefore, the AFM measurements reveal that the geometrical features of HRV can successfully be imprinted into polyurethanes. For the purpose of elucidating the functionality of the respective cavities, we coated dual-channel QCM with such MIP on one side and exposed both channels (with the uncoated one working as a reference) to virus suspensions of the respective species in Tris buffer (pH 7.2). The graph in Figure 2 shows the results obtained with a sensor imprinted with HRV2: after a short tuning period of 15 min to ensure frequency stability of the device, we injected a HRV2 suspension with a concentration of 300 μg/mL. This immediately leads to a frequency decrease of −750 Hz on the imprinted electrode, whereas the frequency only decreases by −100 Hz on the reference channel. The latter represent the amount of viruses interacting with the polyurethane matrix as such (i.e., without templating by HRV). Hence, the difference in response between the two QCM channels can be attributed directly to the imprinting procedure, because this is the only difference in synthesizing the materials, respectively. It adds up to an overall net effect of 650 Hz, proving the substantial amount of sensitivity that can be achieved in this case. Furthermore, the sensor shows both fast response to the injected virus suspension and complete reversibility of the effect, when flushing the measuring cell again with buffer solution. The sensor responses also are dependent on virus concentration: when injecting HRV2 with 150 μg/mL, this leads to half the frequency effects on both electrodes and thus strongly supports linear correlation between a frequency decrease and the analyte concentration. To avoid damaging the template virions

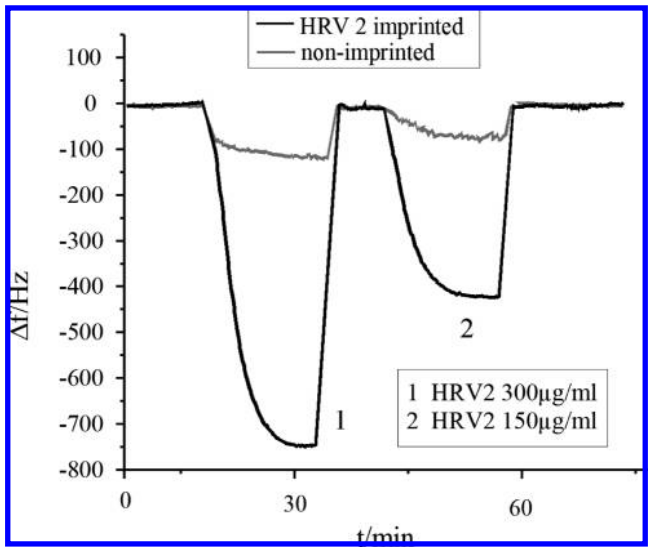

Figure 2. Ten MHz QCM stopped-flow measurements of two differently concentrated HRV2 suspensions with the HRV2 imprinted sensor (measuring temperature = 25 °C).

during imprinting, we applied a modifier (phloroglucinol/phenylenediamin) to each virus stamp to prevent covalent bonds between the HRV surface and possible unreacted isocyanate. Furthermore, if parts of the inner wall of the cavities were covered with the remaining surface proteins, this should lead to a further decrease in the sensor response, because of reduced geometrical fit and the fact that this would somewhat expose the "opposite side" of the surface to the analyte. Besides the material point of view, these results are also very promising in terms of measuring technique: they prove that imprinting leads to artificial matrices that are suitable to be applied as a novel way for fast and cost-effective detection of a virus, for which currently no rapid analytical techniques are feasible. The fast frequency shifts, as well as the fully reversible behavior, furthermore indicate the presence of noncovalent interactions being strong enough for recognition but weak enough to guarantee equilibrium between the sensor layer and the surrounding solution. This is fundamentally different from natural antibodies, because, in that case, binding is much stronger and has a tendency to be irreversible. The large difference in sensor response between the imprint and the reference also clearly indicates that the imprinting procedure is imperative for achieving appreciable sensor results: the layers definitely do not only interact with the viruses by (rather unspecific) noncovalent interactions but at least also need geometrically adapted interaction sites, because we could also observe them, for example, with erythrocytes of different blood groups.[19]

HRV Sensors: Intragroup and Intergroup Selectivity. Selectivity is a key point in designing artificial recognition materials. To assess it in the case of our materials, we initially monitored the modification of virus suspensions after heat treatment. HRV is sensitive to temperature,[20] because VP4 separates from the capsid above 54 °C.[21] However, since VP4 is

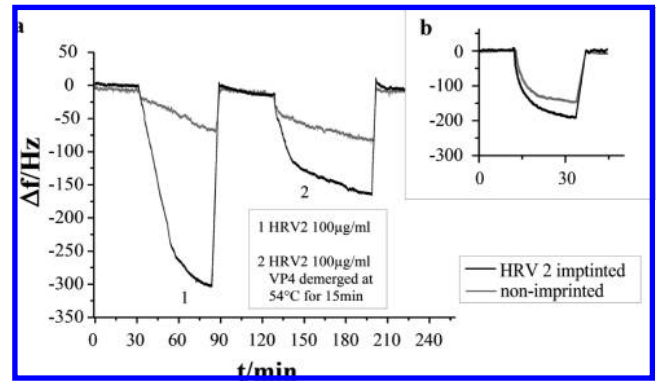

Figure 3. Temperature dependence of the sensor effect, when (a) the virus suspension is heat-treated with 54 °C to demerge VP4, and (b) the virus was denatured by heating up to 60 °C (measuring temperature = 25 °C).

located inside the virion, removing it should only minimally alter the virus surface. Hence, treated viruses should still lead to observable sensor responses. Figure 3a confirms this: for a HRV sample treated at 54 °C for 15 min, the sensor responses are approximately half as large as those for the untreated virus suspension. This fact can be explained by both a conformational change on the virus surface and a decrease in the virion's mass by ~20%. Because the geometry of the particle is generally preserved, the cavities on the sensor surface still incorporate them. Heating the suspension to 60 °C, however, completely denatures the rhinovirus. As a result of this, no more selective mass effects can be observed by the sensors as illustrated in Figure 3b: here, both the imprinted and the nonimprinted channel lead to almost the same frequency shifts. In addition, the effects on the reference electrode increase by a factor of more than two, compared to the untreated viruses. Combining this information with the fact that AFM shows no integral particles in a heat-treated virus suspension, one can conclude that the effects on both the MIP electrode and the reference are caused by unspecific adsorption of protein fragments from the solution onto the polymer surfaces. On the one hand, they lead to smaller sensor responses on the MIP material, because the interaction sites are not optimized for recognizing them. On the other hand, they can more densely occupy the nonimprinted surface, compared to intact viruses. These results lead to the conclusion that two parameters influence the interaction between the virus and the selective layer: both the geometry and the surface chemistry of the sensor layer must be optimized, which leads to adsorption of the virus into the cavities by weak, noncovalent interactions. This then results in noncovalent binding of the virus to the polymer and therefore causes a frequency decrease, according to Sauerbrey's law, even though it is only strictly valid for rigid surfaces. These observations, in principle, also open up the way for a sensor system to be suitable for detecting infectious and noninfectious virions and distinguishing them from each other: the principal way for doing so would be the implementation of a sensor array with three different coatings, namely one nonimprint and one imprint each for active and nonactive species, respectively. The necessary data mining could then be performed by chemometry.

Given these conclusions, it should be possible to distinguish not only between native and denatured forms of the same species—i.e., HRV2—but also between different HRV serotypes.

(19) Hayden, O.; Mann, K.-J.; Krassnig, S.; Dickert, F. L. *Angew. Chem., Int. Ed.* **2006**, *45*, 2626–2629.
(20) Kremser, L.; Bilek, G.; Blaas, D.; Kenndler, E. *J. Sep. Sci.* **2007**, *30*, 1704–1713.
(21) Okun, V. M.; Nizet, S.; Blaas, D.; Kenndler, E. *Electrophoresis* **2002**, *23*, 896–902.

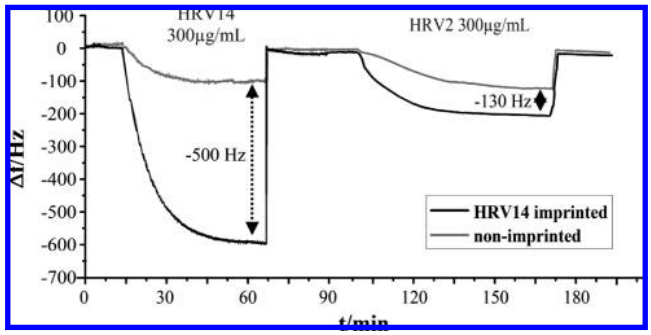

Figure 4. Response of the 10 MHz QCM, coated with polyurethane, HRV14 imprinted when first exposed to a suspension that contained the template and afterward to a suspension of HRV2 with the same concentration (measuring temperature = 25 °C).

In this case, again, the geometrical features of the analyte and the template are the same, but the surface chemistries are not. For this purpose, we investigated the sensor effects for another major group virus, namely, HRV14. Figure 4 illustrates the results: we prepared a MIP from HRV14 and exposed it both to suspensions of HRV14, the template (a), and HRV2 (b). First of all, both measurements show excellent signal-to-noise ratios. Furthermore, the unspecific effects on the reference electrode are approximately the same for both serotypes, which means that basically there is no difference in affinity of the two viruses toward the unmodified polyurethane surface. This fact also confirms that the two rhinovirus representatives are chemically very similar. However, on the MIP material, the effects are completely different: when exposing the sensors to the template serotype (i.e., HRV14), the MIP-coated QCM channel yields a mass effect of 500 Hz, whereas the sensor response to HRV2 is substantially less pronounced, totaling 130 Hz. This difference in selectivity points out the success of the imprinting approach: because the two serotypes are of the same size, the effect caused by geometrical fit between the viruses and the imprinted cavities on the polymer surface should be equal. Therefore, the difference between the effects can be traced back to the fact that imprinting generates active sites that favor the adsorption of the imprinted serotype, because of preorganized noncovalent interaction networks. Even though the competing serotype has the same virion shape, it is bound more weakly. This fact also strongly supports that MIP layers recognize the virus according to its entire outer shell, rather than only according to a specified binding site, such as that observed for natural antibodies binding to the receptor on the surface.

Consequently, this selectivity, globally taking into account the surface properties of the respective template virus, should make it possible to distinguish between any two HRV serotypes independent of which group (major/minor) to which they belong. Therefore, it should be possible to also rationally generate materials with pronounced intragroup selectivity (i.e., sensors for viruses that have the same geometrical features and the same receptor sites). This is a matter of particular interest, because for viruses that belong to the same group (major/minor) and therefore have identical receptors, conventional immunology-based analysis would be difficult. As a sample system, we chose MIPs templated with HRV2 and HRV1A, respectively, both of which are representatives of the minor group, as well as the HRV14 MIP, to compare the results directly with a major group sensor. Analytes include the three templates, as well as HRV16. Furthermore, we

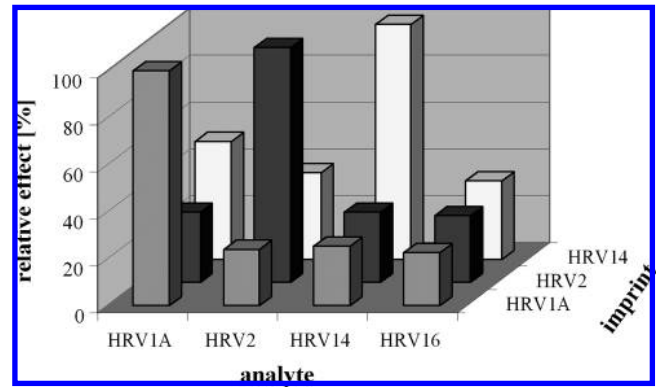

Figure 5. Summarized comparison of the obtained effects with the generated sensors toward various HRV serotypes.

prepared the virus sample suspensions in a way that they lead to net frequency effects of ~300 Hz when exposed to their MIPs (~150 µg/mL). This ensures that the sensor surfaces are not saturated and, hence, all measurements perform well within the dynamic range. Figure 5 summarizes the results of these QCM measurements: first of all, all MIP sensors strongly prefer their own template over all competing species, with selectivity factors usually being in the range of 3−4. For instance, the HRV imprint leads to a net effect (i.e., the difference in frequency shifts between MIP and reference) of −370 Hz, whereas the sensor response toward HRV1A is only −110 Hz. Regarding the similarity of the two serotypes, this difference in the sensor responses is appreciable large, especially when taking into account that the polymer layer represents only a single plate of separation. Generally speaking, intragroup selectivity of each of the imprints is the same as intergroup selectivity: HRV14, HRV16, and HRV2 lead to similar sensor responses with the HRV1A and so on. From the immunological point of view, this is astonishing, because, obviously, the type of receptor site does not have any influence on the sensor signals: on first thought, one would expect higher cross selectivity between serotypes of the same group than between the groups. This strongly supports the assumption that imprinting generates a preformed pattern for noncovalent interactions with the entire virus surface rather than only the receptor site, which, in fact, adds up to only a very small portion of the surface. Thus, unlike an antibody, our MIPs represent artificial antibodies against the entire virus particle.

Interspecies Selectivity. Picornavirus MIP sensors offer the unique possibility of independently assessing the effects geometrical and chemical fit, because they offer a family of different species, consisting of a variety of serotypes within some species. To complement the selectivity studies, we hence also evaluated the cross sensitivity of our MIPs toward another picornavirus representative, namely, the foot-and-mouth disease virus (FMDV).[22] Besides the surface chemistry differing from HRV, FMDV also is smaller, with a diameter of 25 nm,[23] so it does not exactly fit the cavities in the imprinted material. Hence, we exposed a HRV MIP to different virus suspensions that contained HRV and fully deactivated FMDV in the same particle concentration, respectively. This, of course, does not correspond to the same

(22) Grubman, M. J.; Baxt, B. *Clin. Microbiol. Rev.* **2004**, *17*, 465–493.
(23) Acharya, R.; Fry, E.; Stuart, D.; Fox, G.; Rowlands, D.; Brown, F. *Nature* **1989**, *337*, 709–716.

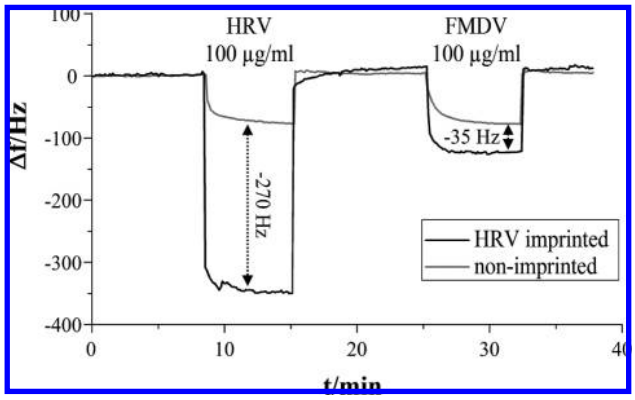

Figure 6. Comparison of the frequency responses of the 10 MHz QCM, coated with polyurethane and imprinted with HRV toward suspensions of HRV and FMDV, respectively, showing a net effect of only −35 Hz for the nontemplate virus (measuring temperature = 25 °C).

mass concentration, because of the different molecular weights. Doing so is reasonable, because, in this way, the amount of particles in the solution and the amount of interaction sites in the sensitive layer is always the same, therefore leading to similar kinetics, which are mainly diffusion-controlled in these systems. An example result can be seen in Figure 6: evidently, the mass effect on the QCM—i.e., the difference between the MIP and the reference—is only −35 Hz for the FMDV, whereas the HRV leads to a frequency shift of −270 Hz. In this case, the HRV MIP was prepared with HRV2 as a template. Both virus suspensions contained 100 μg/mL of the respective virus species in the aforementioned buffer. Compared to intergroup and intragroup selectivities of the HRV, the selectivity factor increases by a factor of ∼9. Thus, cross-sensitivity is a factor of 3 lower than that between different HRV species. This effect is clearly related to the imprinting procedure, because the nonspecific effects on their reference electrode are the same for both HRV and FMDV. The small additional mass effect of the MIP material toward FMDV shows that the virus occupies a small portion of the interaction centers present. However, because of the difference in size between the particle and the cavity, binding is by far not optimal, resulting in an additional mass effect, reaching only ∼50% of the nonspecific interaction. Again, these results demonstrate the chemical relationship between the two picornaviruses and, hence, show the high selectivity accessible throughout the imprinting method.

Interaction Isotherm—Binding Properties. The adsorption isotherm of the smallest picornavirus FMDV, serotype Manissa, is shown in Figure 7a. This serotype has the smallest diameter of these species (only 25 nm). A steep slope is obtained at the beginning and then the curvature decreases in parallel with concentration enhancement. This is a typical example of multisite adsorption with privileged interaction sites followed by less favorable adhesion. The lack of saturation with plateau indicates that the simple Langmuir model is not valid. For MIPs, often, the Freundlich isotherm[24] is proposed, which usually refers to small analyte molecules. According to physical adsorption phenomena, the BET model is preferably suitable for gases at porous materials.

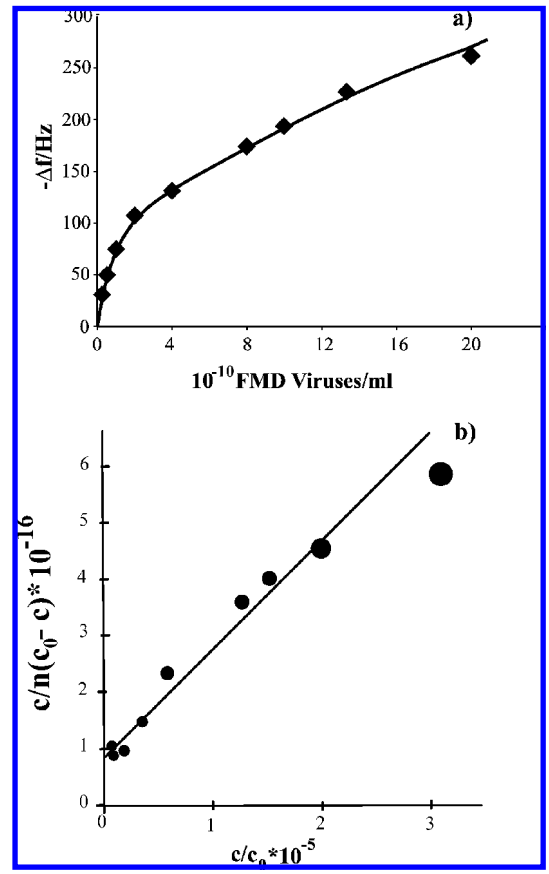

Figure 7. (a) 10 MHz QCM sensor characteristic of the Manissa FMD virus using MIP coating at 25 °C. (b) Linearized BET adsorption isotherm of Manissa FMD virus on MIP at 25 °C, according to eq 1 (correlation coefficient of linear regression, $R^2 = 0.96$).

BET analysis is highly favorable, because of the physical interpretation, according to multisite adsorption.[25] A monolayer must be considered, yielding a high interaction energy, followed by less-favorable adsorbates. The BET equation can be derived by considering energy differences according to the Boltzmann exponential factor ($\exp[-\Delta E/(RT)]$), the interaction energy (ΔE), the thermal energy (RT), and the exchange rates between different sites. As in the case of adsorption of inert gases, van der Waals interactions and other noncovalent phenomena are also valid for viruses. One must only consider that the pressure of the pure gas (p_0) must be substituted by the most densely packed virus concentration (c_0), and the partial pressure p must be substituted by the virus concentration c in aqueous solution:

$$\frac{c}{n(c_0 - c)} = \frac{1}{n_m b} + \frac{b-1}{n_m b}\left(\frac{c}{c_o}\right) \qquad (1)$$

This equation can be considered to be the linearized BET isotherm for viruses. The number of adsorbed viruses in the sensor layer (n) can be derived by the frequency shift of the sensor, their volume, their density, and the sensitivity of the QCM, which corresponds to 0.6 Hz/ng. This mass-sensitivity results from calibration measurements that are conducted with poly(vinyl chloride) that has almost the same

(24) Rampey, A. M.; Umpleby, R. J., II; Rushton, G. T.; Iseman, J. C.; Shah, R. N.; Shimizu, K. D. *Anal. Chem.* **2004**, *76*, 1123–1133.

(25) Dickert, F. L.; Haunschild, A.; Kuschow, V.; Reif, M.; Stathopoulos, H. *Anal. Chem.* **1996**, *68*, 1058–1061.

density as the virus.[26] The parameter n_m describes the number of privileged sites in the layer. The parameter b is given as

$$b = \exp\left(\frac{\Delta E}{RT}\right)$$

where energy ΔE is the difference of interaction energies between favorable and less-favorable binding sites.[25]

Figure 7b shows the linearized BET plot resulting from the FMDV sensor characteristic depicted in Figure 7a and eq 1. From the slope and the intercept, the n_m value can be derived as being $n_m = 6.9 \times 10.^{10}$ At the highest concentration measured, the overall mass effect is 265 Hz, which corresponds to 5.4×10^{10} virions bound to the sensitive layer. Obviously, the decreasing slope in the sensor characteristic indicates the onset of saturation, because the number of the incorporated viruses reaches 78% of the available favorable binding sites. Parameter b (eq 1) leads to an energy difference of 29 kJ/mol between favorable and disfavorable binding sites in the MIP layer. Compared to small molecules, such as chloroform,[25] this value is higher by a factor of 3.5, because of the substantially larger interaction area.

CONCLUSION

Molecular imprinting leads to artificial receptors for the selective interaction with picornaviruses, as we could show with the example of the human rhinovirus (HRV) and the foot-and-mouth disease virus (FMDV). Molecularly imprinted materials reversibly reincorporate these virus species and, hence, can be applied for recognition in chemical sensing (e.g., in combination with a mass-sensitive transducer such as the quartz crystal microbalance). Besides opening up a feasible pathway to the rapid analysis of viruses for the first time, the resulting molecularly imprinted polymer (MIP) materials are also excellently suited to study the influence of both geometry and surface chemistry on the interaction behavior of the respective recognition material: selectivity studies between different HRV serotypes revealed that the MIP prefers the template species by a factor of 3−4. This is the case for both HRV that belongs to the same group (major/minor) as the template and for species of different groups. Hence, in contrast to natural antibodies, the entire surface is recognized by the MIP, because the larger difference in receptor site chemistry between the major group and the minor group does not have any role at all. If, additionally, the geometry is also not exactly fitting (such as in the case of the FMDV), cross-sensitivity of HRV MIP decreases by another factor of 3. Because weak noncovalent interactions play the main role during recognition, this can be modeled quantitatively by a BET isotherm, yielding the number of favorable interaction sites.

Received for review September 16, 2008. Accepted May 5, 2009.

AC8019569

(26) Rowlands, D. J.; Sangar, D. V.; Brown, F. *J. Gen. Virol.* **1971**, *13*, 141–152.